BAMS Article

Observing the Diurnal Cycle of Coastal Rainfall over Western Puerto Rico in Collaboration with University of Puerto Rico Students

Rosimar Rios-Berrios, Naoko Sakaeda, Héctor J. Jimenez-González, Angelie Nieves-Jimenez, Yidiana Zayas, Elinor Martin, Shun-Nan Wu, Cameron R. Homeyer, and Ernesto Rodríguez

ABSTRACT: The diurnal cycle of coastal rainfall over western Puerto Rico was studied with high-frequency radiosondes launched by undergraduate students at the University of Puerto Rico at Mayagüez (UPRM). Thirty radiosondes were launched during a 3-week period as part of NASA's Convective Processes Experiment—Aerosols and Winds (CPEX-AW) field project. The objective of the radiosonde launches over Puerto Rico was to understand the evolution of coastal convective systems that are often challenging to predict. Four different events were sampled: 1) a short-lived rainfall event during a Saharan air dust outbreak, 2) a 2-day period of limited rainfall activity under northeasterly wind conditions, 3) a 2-day period of heavy rainfall over land, and 4) a 2-day period of long-lived rainfall events that initiated over land and propagated offshore during the evening hours. The radiosondes captured the sea-breeze onset during the midmorning hours, an erosion of lower-tropospheric inversions, and substantial differences in column humidity between the four events. All radiosondes were launched by volunteer undergraduate students who were able to participate in person, while the coordination was done virtually with lead scientists located in Puerto Rico, Oklahoma, and Saint Croix. Overall, this initiative highlighted the importance of student–scientist collaboration in collecting critical observations to better understand complex atmospheric processes.

KEYWORDS: Rainfall; Coastal meteorology; Radiosonde/rawinsonde observations; Education

https://doi.org/10.1175/BAMS-D-21-0322.1

Corresponding author: Rosimar Rios-Berrios, rberrios@ucar.edu

In final form 22 October 2022

AFFILIATIONS: Rios-Berrios—National Center for Atmospheric Research, Boulder, Colorado; **Sakaeda, Martin, Wu, and Homeyer**—School of Meteorology, University of Oklahoma, Norman, Oklahoma; **Jimenez-González, Nieves-Jimenez, and Zayas**—Universidad de Puerto Rico, Recinto Universitario de Mayagüez, Mayagüez, Puerto Rico; **Rodríguez**—San Juan Weather Forecast Office, National Weather Service, San Juan, Puerto Rico

The diurnal cycle is one of the fundamental modes of atmospheric variability in the tropics that explains a dominant fraction of rainfall variability, especially over tropical continents and islands (Yang and Slingo 2001; Kikuchi and Wang 2008). Despite its importance, general circulation models struggle to simulate the observed diurnal behavior of tropical rainfall (Dirmeyer et al. 2012; Dias et al. 2018; Christopoulos and Schneider 2021; Watters et al. 2021). The diurnal cycle of rainfall is further complicated by land–sea interactions and topography over tropical islands and coastal regions (Biasutti et al. 2012; Smith et al. 2012; Ruppert et al. 2020). Western Puerto Rico is an example of such regions where the strong diurnal cycle of rainfall is observed but its prediction remains challenging. About two-thirds of the daily rainfall happens around 1400–1700 local time (LT) (Jury 2022), but the precise location of the heaviest rainfall can vary from day to day (Jury et al. 2009; Jury and Chiao 2013; Villamil-Otero et al. 2015). To better understand the complex factors that modulate the diurnal cycle of precipitation in Puerto Rico, radiosondes were launched to collect needed observations as part of the National Aeronautics and Space Administration (NASA)'s Convective Processes Experiment—Aerosols and Winds (CPEX-AW) field campaign. This article provides an overview on the observed events and the collaborative effort between the science investigators and local participants that led to a successful research and educational activity.

A unique characteristic of Puerto Rico is its east–west-oriented central mountain range (known in Spanish as the "Cordillera Central"). Figure 1 shows that mountain range through a map of elevation above sea level. The mountainous region is characterized by elevations exceeding 0.5 km, with some local peaks reaching elevations above 1 km within the central interior region of the island. Such topography modulates the predominant southeasterly flow around and within the island, leading to climatological rainfall maxima in the western interior and rainfall minima in the southwestern region (Larsen 2000; Fernández-Alvarez et al. 2020; Jury 2022). The climatological rainfall maxima in the western interior is mostly contributed by convection that typically develops in the early afternoon. The afternoon convection then often moves northwestward as it dissipates by late afternoon.

Daily weather discussions provided by the National Weather Service (NWS) in San Juan frequently quote the "diurnal cycle" and "local effects" as potential triggers of afternoon thunderstorms. Those local effects include the complex island topography in combination with sea-breeze circulations that form by late morning associated with temperature contrasts between the island and its surrounding water. This sea breeze is thought to contribute to the afternoon initiation of convection through its landward flux of moisture and near-surface convergence with topography and background southeasterly trade winds (Jury et al. 2009; Jury and Chiao 2013; Villamil-Otero et al. 2015).

Although this typical behavior of the diurnal cycle is well-known by the locals, there is large day-to-day variability in how the afternoon convection develops and evolves. For example, on

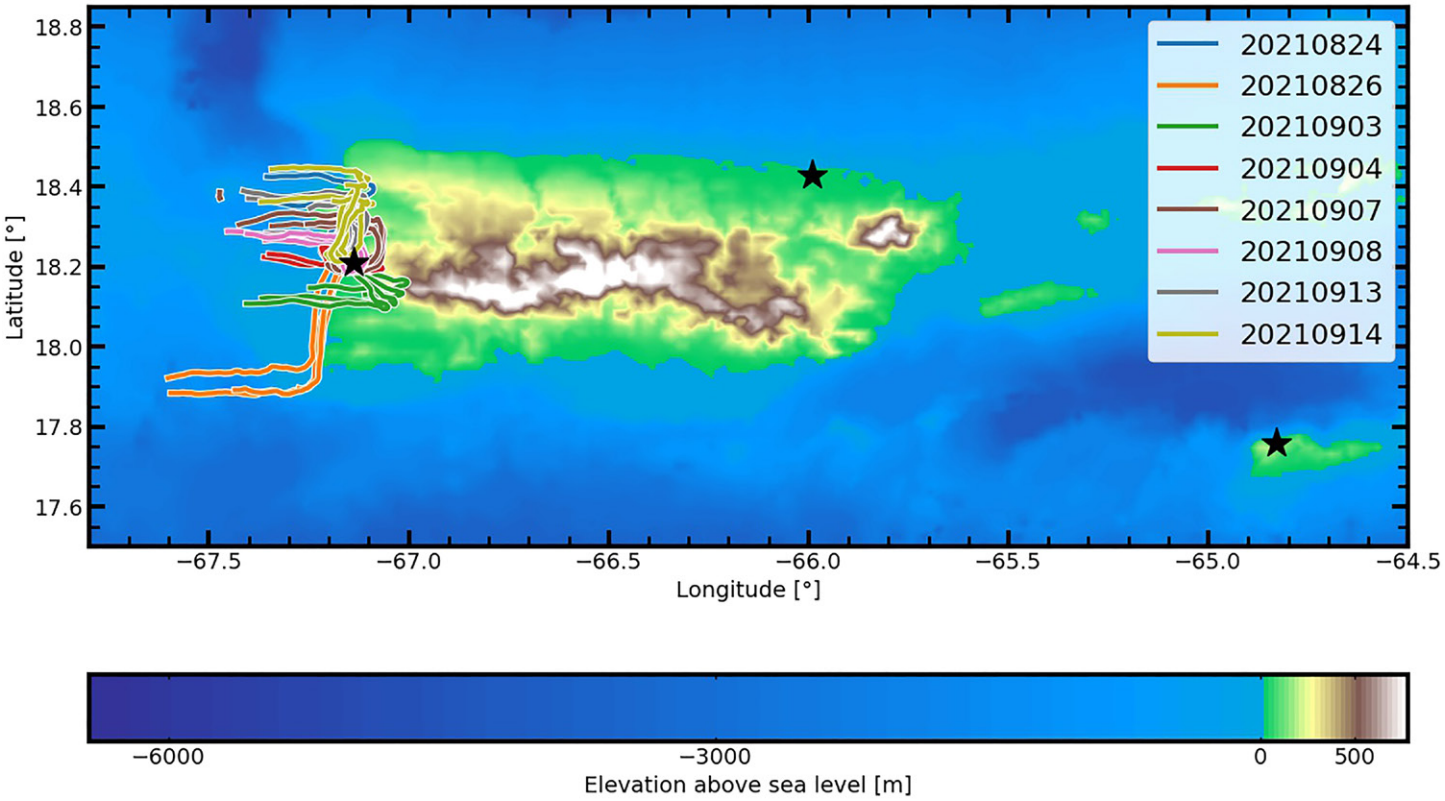

Fig. 1. Map showing our region of study, elevation (shading), and the trajectories of all radiosondes launched. The trajectories are colored by date according to the legend. Stars show the location of the UPRM campus (westernmost star), the location of the NWS WFO San Juan (northernmost star), and the main operations center for CPEX-AW in Saint Croix (easternmost star).

some days, the afternoon convection remains isolated and dissipates quickly. In contrast, other days may be characterized by convection growing upscale and continuing to propagate offshore. These are just some examples of variability, and the diurnal evolution of rainfall can vary in other ways such as its propagation direction, structure, and timing. Predicting the precise behavior can often be challenging for the local weather forecasters. This challenge results (at least partly) from an incomplete understanding of convection initiation, development, and propagation near coastlines. Given that there are currently no observations that resolve the diurnal cycle of the atmospheric profile over western Puerto Rico, targeted observations through field campaigns are critical to advancing our understanding of coastal diurnal rainfall.

To improve our understanding and prediction of the diurnal cycle of rainfall over western Puerto Rico, high-frequency radiosondes were launched as part of NASA's CPEX-AW field campaign during August and September 2021. CPEX-AW was part of the international Joint Aeolus Tropical Atlantic Campaign (JATAC) between NASA and the European Space Agency (ESA). The objectives of JATAC included calibrating and validating ESA's *Aeolus* satellite lidar, as well as improving the understanding of tropical convective systems and their interactions with the Saharan air layer. These objectives were pursued through the collection of airborne and in situ observations from Cape Verde and Saint Croix. The operational center of CPEX-AW was situated in Saint Croix (easternmost star in Fig. 1), where flights were coordinated to collect observations with NASA's DC-8 aircraft. An additional team was deployed to Mayagüez, Puerto Rico (westernmost star in Fig. 1), to launch radiosondes on targeted days when convection was expected to form over the region. The scientific objectives and launching strategies will be discussed in the second section.

CPEX-AW coincided with a time of global restrictions and uncertainty due to the COVID-19 pandemic. While some CPEX-AW participants were able to join the field campaign in person, not every participant was able to do so. At the same time, the project took place in highly

populated islands where local residents and weather forecasters experience the rainfall themselves. For these two reasons, our team included a meaningful collaborative partnership between CPEX-AW participants, local students and professors at the University of Puerto Rico at Mayagüez (UPRM), and NWS San Juan forecasters. Daily coordination to decide on radiosonde launches included conversations among all team members. On targeted dates, the radiosondes were launched by undergraduate students and their professors from the rooftop of the Physics Department building at UPRM. The students also experienced the data collection from deciding on which day to launch radiosondes to monitoring the data in real time. This collaborative approach—including local residents and forecasters—was critical to successfully use the limited radiosondes on days of convective activity while also allowing us to complete our project during the global pandemic.

Scientific and educational tools

Radiosondes. The scientific objective of the radiosonde launches was to capture the diurnal cycle of atmospheric profiles near the western coastline of Puerto Rico. To capture the diurnal cycle, four to five radiosondes were launched on eight targeted days between 26 August and 14 September 2021. Radiosonde launches often included one morning launch to take atmospheric measurements prior to the sea-breeze onset, one launch around noon to capture the early-stage depth and intensity of the sea breeze, another launch in the early afternoon to sample the atmospheric conditions during convective development, and a last launch during the late afternoon to capture the postconvective environment. All radiosonde launches took place in the UPRM campus for consistency across the different days sampled.

We used iMet-4 radiosondes from International Met System and a ground station that has been built for ozonesondes at the University of Oklahoma (https://homeyer.oucreate.com/ozonesondes/), except that the ozone sensors were not included in our launches. This ozonesonde ground station was built following the guidelines publicly provided by the NOAA Earth System Research Laboratory Global Monitoring Laboratory (https://gml.noaa.gov/ozwv/wvap/sw.html). The use of the preexisting ozonesonde system had the benefit of eliminating the cost of developing a new system. The iMet-4 radiosondes provide measurements of temperature, humidity, pressure, wind speed, and wind direction with an uncertainty of 0.5–1 K, 5%, 0.5–2 hPa, 0.5 m s^{-1}, and 1°, respectively. All radiosonde data were quality controlled using the Atmospheric Sounding Processing Environment (ASPEN) software (Martin and Suhr 2021), which was developed and supported by the Earth Observing Laboratory of the National Center for Atmospheric Research (NCAR). The quality controlled data are freely available via NASA's data archive (Jackson 2022).

NWS forecasts. When deciding on a worthy event to sample, our team heavily relied on the local weather forecasters. The decision of when to launch was made 1–3 days before the event to allow time for the students to plan their schedules around their coursework. To make such decisions, our main source of information was the local weather forecast provided by the NWS San Juan Forecast Office. Among their products, the NWS San Juan office provided an experimental ensemble-based rainfall product with likely daily accumulations for the following three days. We decided to launch radiosondes when that forecast product showed accumulated rainfall over the western coast of Puerto Rico. We also discussed the forecast in further detail through direct communication with NWS San Juan weather forecasters. Besides providing their input on our sampling strategies, the forecasters pointed out days of higher-than-usual uncertainty. This collaboration further reinforced our decision of when to launch the radiosondes to understand the conditions behind forecast challenges. All sounding data were sent to the forecasters shortly after the radiosonde reached the tropopause. Some forecasters used the information when updating their daily forecasts (e.g., noticing the removal

of capping inversions), highlighting the meaningful two-way collaboration built as part of this project.

Model forecasts. Our team also relied on numerical weather prediction models to select the day and frequency of radiosonde launches. A unique tool available to us was real-time model output from several convection-permitting modeling systems configured by CPEX-AW team members. Those models included the Unified Wave Interface-Coupled Model (provided by Prof. Shuyi Chen from the University of Washington), two versions of the Weather Research and Forecasting (WRF) Model with data assimilation (provided by Prof. Zhaoxia Pu from the University of Utah) and aerosols capabilities (provided by Prof. Shu-Hua Chen from the University of California, Davis), and the Model for Prediction Across Scales–Atmosphere (MPAS-A) (Skamarock et al. 2012) (provided by NCAR). Our team mostly used model output from MPAS-A, which is a global model with grid refinement capability. MPAS-A was integrated in real time during August–September 2021 in support of CPEX-AW using a global domain and a refined region with 3-km cell spacing over most of the Atlantic Ocean (Fig. 2a). The domain then transitioned to 15-km cell spacing elsewhere. The region of highest horizontal resolution included the oceanic domain sampled by NASA's DC-8 aircraft as well as western Puerto Rico.

In spite of being a global model, MPAS-A captured the daily sea-breeze circulation over western Puerto Rico. Figures 2b and 2c show simulated reflectivity, 10-m wind speed, and mean sea level pressure as examples depicting the sea breeze and associated rainfall forecast from MPAS-A. The sea-breeze circulation is evident by the onshore (i.e., westerly) flow over western Puerto Rico. Most of the forecast rainfall is located near a convergence zone and a cyclonic feature over northwestern Puerto Rico. This type of forecast is consistent with previous analyses of rainfall events associated with sea-breeze and orographic circulations over western Puerto Rico (Jury et al. 2009; Villamil-Otero et al. 2015). The global domain also

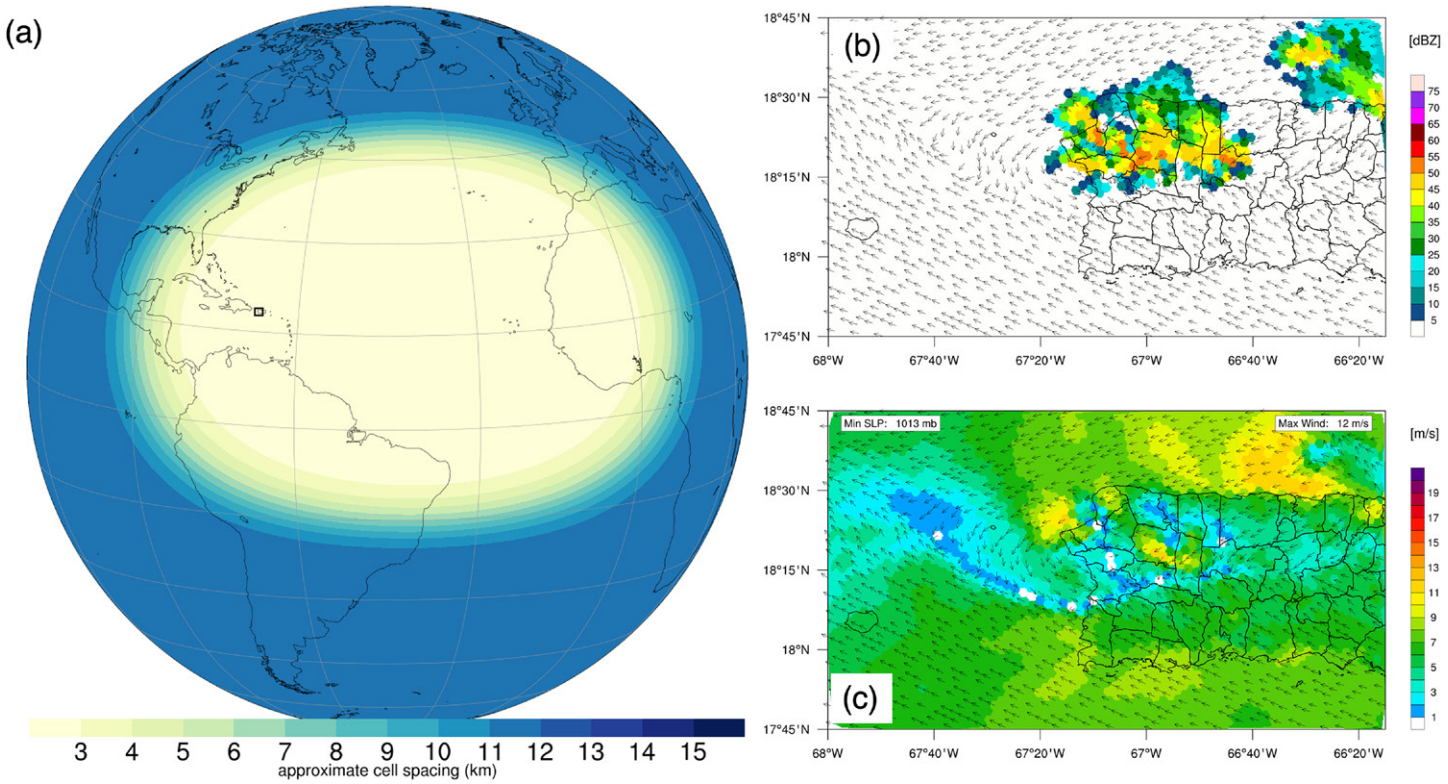

Fig. 2. (a) Global map showing the approximate horizontal cell spacing of the MPAS-A forecasts used in support of our study. (b),(c) Illustrative examples of a sea-breeze circulation and associated rainfall in a 41-h MPAS-A forecast initialized at 0000 UTC 13 Sep 2022. The plot in (b) shows 1-km reflectivity (shading; every 5 dBZ) and 10-m wind vectors (arrows). The plot in (c) shows 10-m wind speed (shading; every 1 m s^{-1}) and 10-m wind vectors (arrows).

ensured that large-scale synoptic features—including the North Atlantic subtropical high, upper-tropospheric troughs, and tropical cyclones—were captured within the model domain. Given these benefits, we used MPAS-A forecasts as additional sources of information to decide on days to launch radiosondes. A future study will use the MPAS-A forecasts, in combination with the radiosonde data presented herein, to augment our analysis of the diurnal cycle of rainfall in western Puerto Rico.

Accomplishments

Sampled events. We launched 31 radiosondes during our campaign, out of which 29 launches were successful. All of the 29 successful launches reached the tropopause, although the precise path there varied from event to event. Figure 1 shows the different tracks followed by the radiosondes. Additionally, Fig. 3 shows the synoptic configuration from select days based on maps of atmospheric conditions in the ERA5 product (Hersbach et al. 2020). On most days, the radiosondes moved inward toward the central mountain range and northward toward the northwestern coast, followed by a westward turn after reaching the tropopause. Exceptions happened on 26 August and 3–4 September, when the radiosondes traveled southward before making their westward turn. The pattern on 26 August was influenced by the upper-tropospheric outflow of a developing cyclone in the western Caribbean, which became Tropical Storm Ida later on that day (Fig. 3a). On 3–4 September, the upper-tropospheric flow was responding to an approaching weak easterly wave (Fig. 3b).

The successful radiosonde launches covered different portions of the diurnal cycle (Fig. 4). Four radiosonde launches happened during the early morning hours between

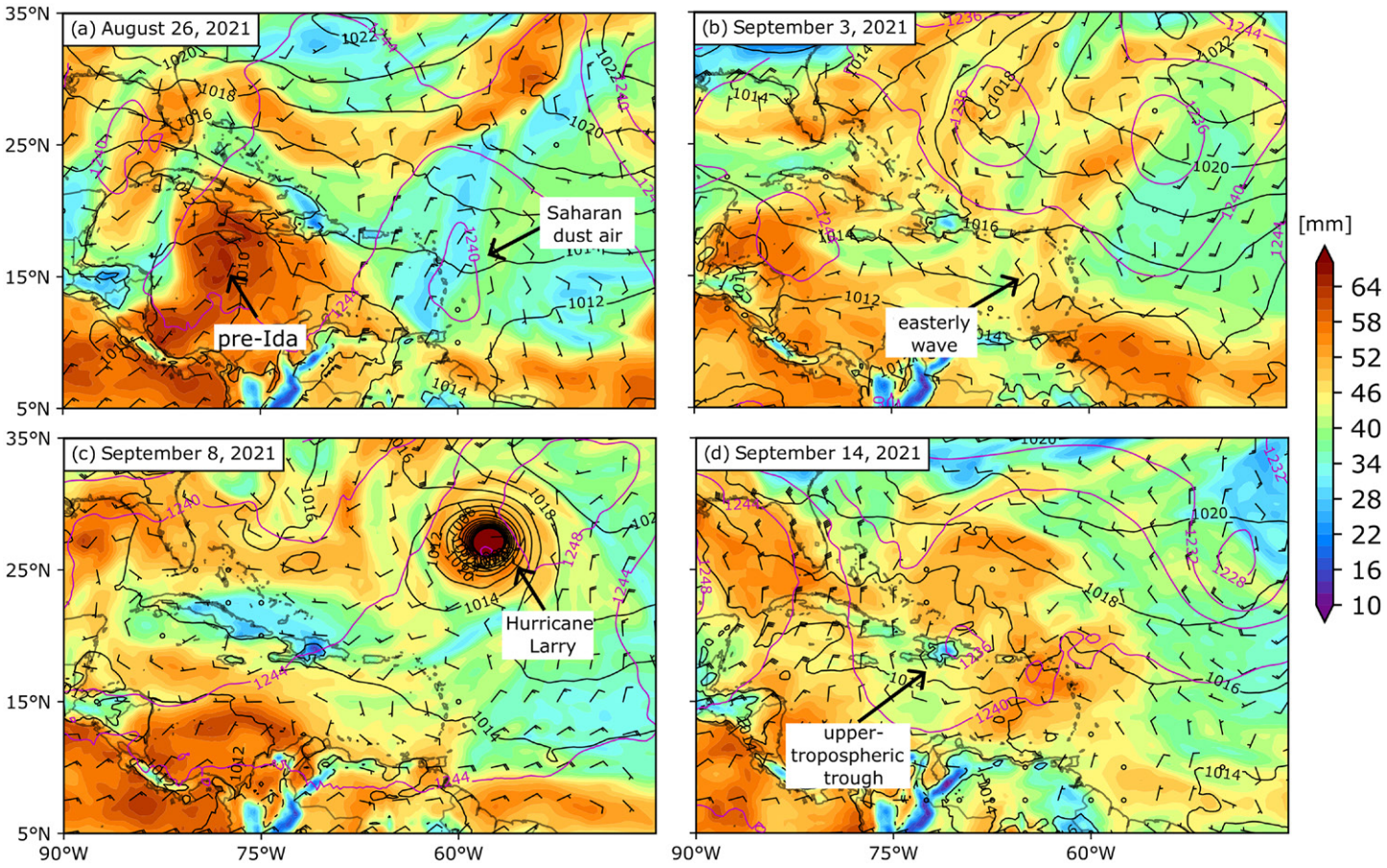

Fig. 3. Horizontal maps of synoptic conditions at 0800 LT (1200 UTC) (a) 26 Aug, (b) 3 Sep, (c) 8 Sep, and (d) 14 Sep. Panels show precipitable water (shading; every 1 mm), mean sea level pressure (black contours; every 2 hPa), 200-hPa geopotential heights (magenta contours; every 4 dam), and 200-hPa winds (wind barbs) from the ERA5 dataset (Hersbach et al. 2020).

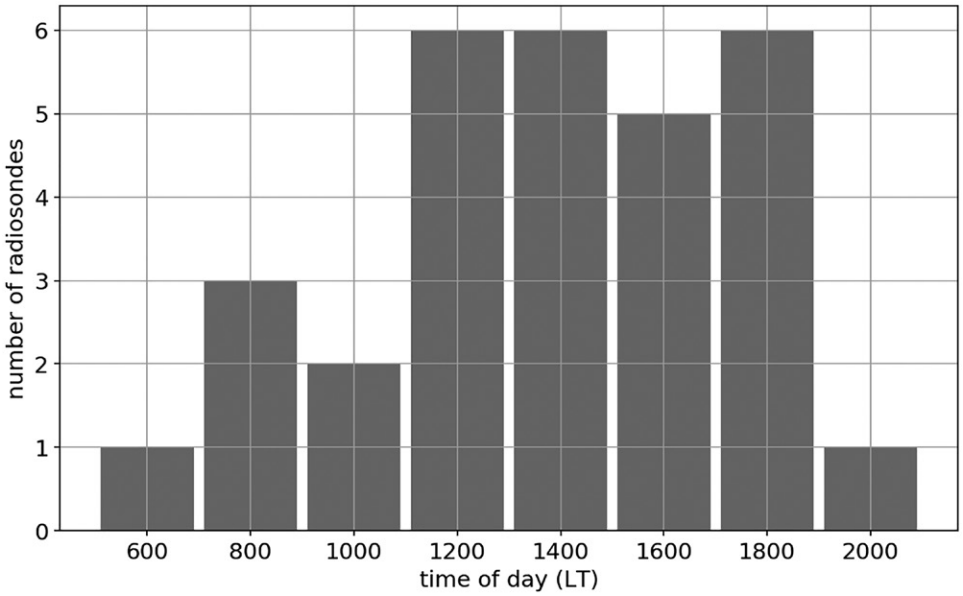

Fig. 4. Histogram showing the number of radiosondes launched from UPRM during 2-h windows.

0600 and 0800 LT. These launches happened on all sampled days between 26 August and 8 September. Most of radiosondes were launched before, during, and after the development of thunderstorms in western Puerto Rico. Two radiosondes were launched at 1000 LT, while six radiosondes were launched every 2 h between 1200 and 1800 LT. Last, there was a single radiosonde launched around 2000 LT during an event of prolonged coastal rainfall.

Figures 5a–d show skew *T* diagrams of the morning radiosondes launched from UPRM and from the NWS San Juan Forecast Office (SJU). There is strong agreement between the temperature and dewpoint from both sources. On 26 August, both the UPRM and SJU soundings show several inversions in the temperature profiles together with a layer of dry air above 800 hPa (Fig. 5a). This dry air was associated with a Saharan dust outbreak over the Caribbean and eastern Atlantic (Fig. 3a). Those conditions changed on 3 September, when "onion-shaped" soundings (Zipser 1977) showed the presence of two dry-air layers separated by nearly saturated conditions around 600 hPa (Fig. 5b). "Onion-shaped" soundings have been observed in the past in association with mesoscale subsidence above a relatively moist layer (e.g., Zipser 1977). Similar conditions were present on 4 September (not shown). Several days later conditions had changed again, and both the UPRM and SJU soundings from 7 to 8 September (Figs. 5c,d) captured several inversions and a dry air mass again above 800 hPa. This dry air was located in the far environment of Hurricane Larry (Fig. 3c).

A major shift in the weather conditions occurred during the last week of our project. The Saharan air dust diminished in the region; instead, multiple tropical cyclones formed over the Atlantic ocean (Fig. 3c) and an upper-tropospheric trough moved over the Hispaniola on 13–14 September (Fig. 3d). The combination of anomalous moist conditions and anomalous southerly flow brought moist and unstable conditions to Puerto Rico. The SJU soundings showed much more humid air—especially in the middle and upper troposphere—on 13–14 September than any of the other days considered (Figs. 5e,f). For example, the dewpoint temperature at 400 hPa was approximately –20°C on 14 September in comparison to approximately –30° to –40°C on other days.

These large-scale conditions likely played a role on the timing, intensity, and longevity of coastal rainfall over western Puerto Rico. Studies over the Maritime Continent and other tropical islands have shown that large-scale disturbances, such as the Madden–Julian oscillation and convectively couple equatorial waves, influence the diurnal cycle of rainfall

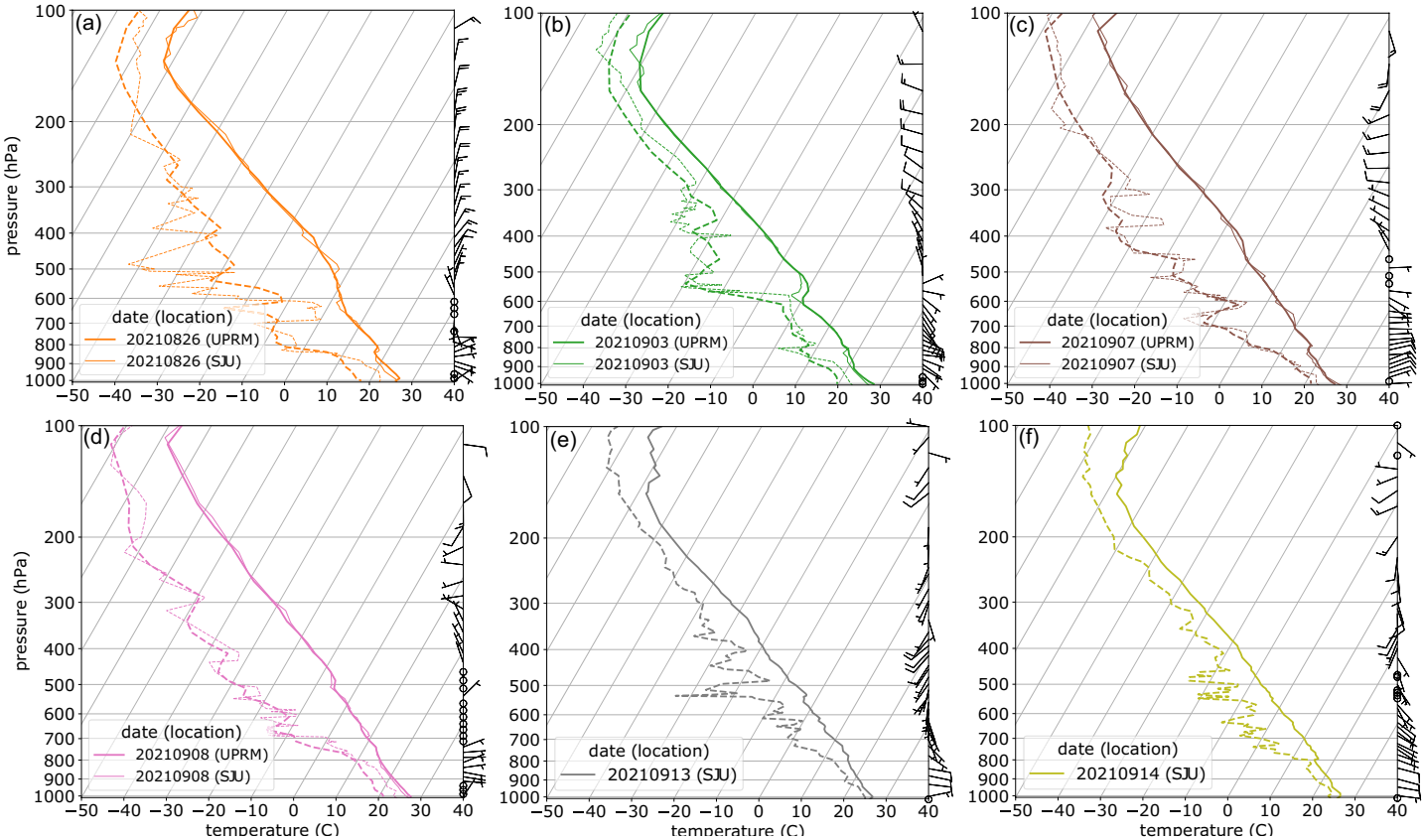

Fig. 5. Skew *T* diagrams showing the morning conditions at UPRM (thick lines) and San Juan (SJU; thin lines). Panels show the soundings launched around 0800 LT (1200 UTC) (a) 26 Aug, (b) 3 Sep, (c) 7 Sep, (d) 8 Sep, (e) 13 Sep, and (f) 14 Sep. The line colors for each day correspond to the same colors and dates in Fig. 1.

due to imposed perturbations on wind and humidity (e.g., Sakaeda et al. 2020; Natoli and Maloney 2021; Bai and Schumacher 2022). In spite of the seemingly unfavorable conditions for sustained rainfall on some days, Puerto Rico still received measurable rainfall on all of the days when we launched radiosondes. This likely points at the role of the diurnal cycle—in conjunction with local effects such as topography and sea-breeze circulations—in promoting the development of rainfall-producing storms over Puerto Rico as noted over other tropical islands (Qian 2020; Zhou et al. 2022). While a detailed study is necessary to investigate that possibility, the following section will present an overview of four select events that occurred under the different flow regimes (Fig. 3). We will use the radiosonde data to characterize the diurnal evolution of atmospheric conditions, but it is possible that some changes happened due to adjustments to convective activity in the region.

26 August event. A relatively weak and localized rainfall event was observed on 26 August 2021. Accumulated rainfall estimates from NOAA's Stage-IV product indicate that approximately 30 mm (1.5 in.) of rainfall fell over the northwestern interior towns of Puerto Rico (Fig. 6a). This event was relatively short lived. Cumulonimbus clouds were first observed by our team around 1300 LT. The local WSR-88D detected storms beginning around 1400 LT and dissipating by around 1700–1800 LT.

Figures 6b and 6c show the evolution of temperature, water vapor, and winds as measured by our radiosondes. As noted above, the morning sounding (0800 LT) shows an inversion around 800-hPa [approximately 1.5 km above ground level (AGL)] and relatively dry conditions aloft. The derived relative humidity was around 55% from the surface up to 800 hPa and around 20% above 800 hPa. Relatively weak easterly winds existed in the lower troposphere while predominantly northerly winds were measured above 500 hPa. This northerly

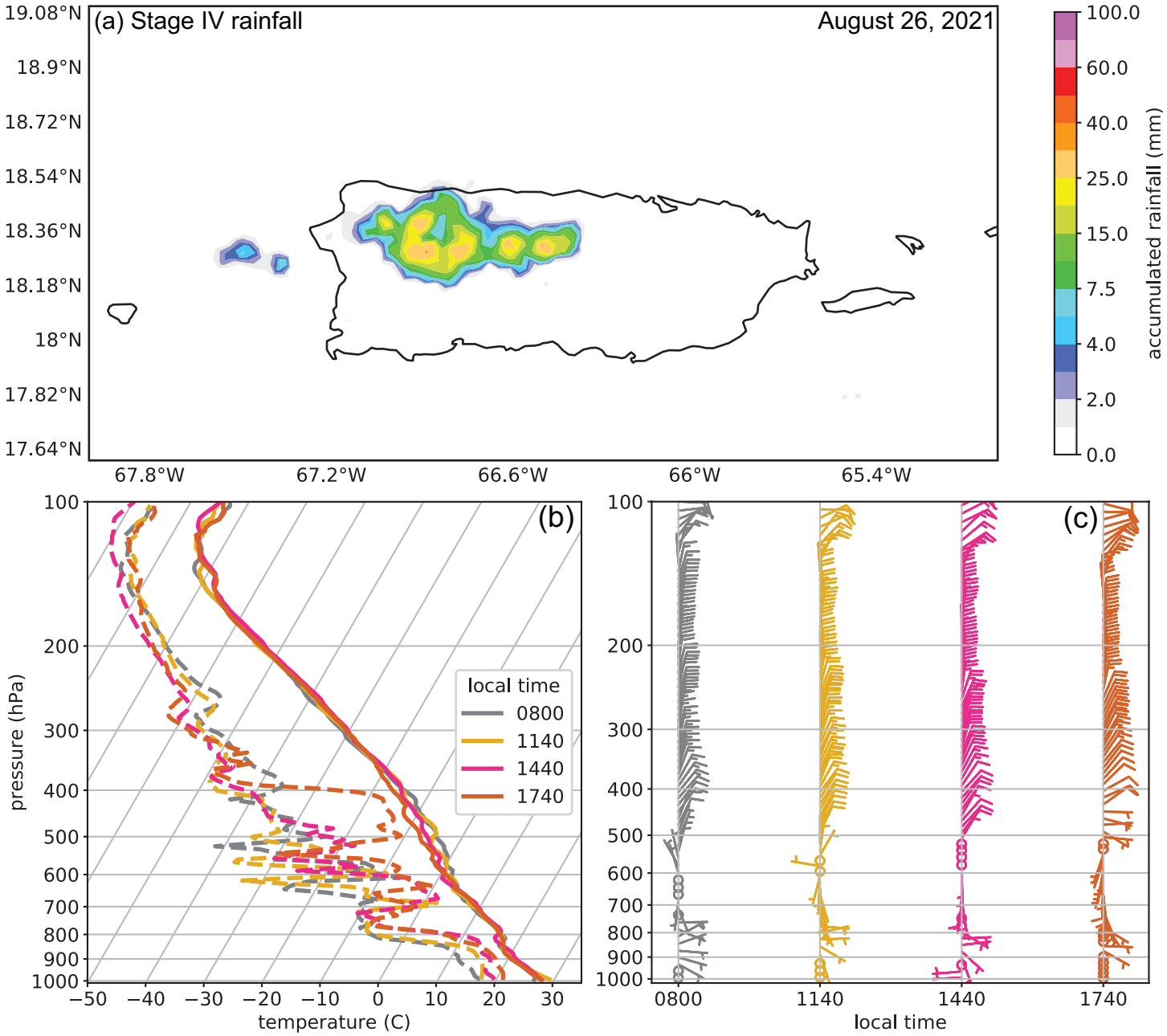

Fig. 6. Summary of observed conditions during the 26 Aug event. (a) 24-h accumulated precipitation from 0800 LT (1200 UTC) 26 Aug until 0800 LT 27 Aug. (b) Skew *T* diagrams of UPRM soundings and (c) vertical profiles of horizontal winds by launch time. Lines and wind barbs are colored according to the time of day, as indicated by the legend in (b).

flow and relatively dry conditions above 500 hPa persisted throughout the day as indicated by the soundings.

Several atmospheric conditions changed throughout the course of this day leading to the rainfall event. By 1140 LT, the surface had warmed up and the boundary layer moistened as indicated by the larger dewpoint temperature in comparison to the morning conditions (Fig. 6b). This moistening contributed to a slight increase in column water vapor as measured by the sounding-derived precipitable water (Fig. 7a). A sea-breeze circulation had initiated by this time as well, which is evident by the near calm conditions between 900 and 1,000 hPa and the southeasterly flow just above 900 hPa (Fig. 6c). Middle-tropospheric temperatures had also cooled down by this time; however, there was no notable increase in instability at this hour as measured by the sounding-derived convective available potential energy (CAPE) (Fig. 7b). Instead, the amount of convective inhibition (CIN) increased in comparison to the morning conditions (Fig. 7c).

As the day progressed, the near-surface temperature continued to increase and the boundary layer continued to moisten. This moistening was likely associated with the strengthening onshore flow as indicated by westerly winds measured by the 1440 LT sounding (Fig. 6b). Also at that time, the precipitable water increased to approximately 35 mm and CAPE increased to approximately 100 J kg^{-1} (Figs. 7a,b). Despite such increases, conditions remained relatively unfavorable for prolonged storm development during the time of peak convergence associated with the onshore flow and the upstream easterlies. By the early evening hours, the 1740 LT sounding measured the largest amount of boundary layer moisture, column precipitable water, and CAPE on this day. However, the middle troposphere remained dry (except for a moist layer between 400 and 500 hPa likely associated with clouds) and the sea-breeze circulation had weakened as indicated by near calm conditions (Fig. 6c). These data suggest that increased instability, boundary layer moistening, and inland convergence aided by the sea breeze contributed to the formation of storms on this day, but the exceptionally dry middle-tropospheric conditions limited the lifetime of storms and the amount of precipitation.

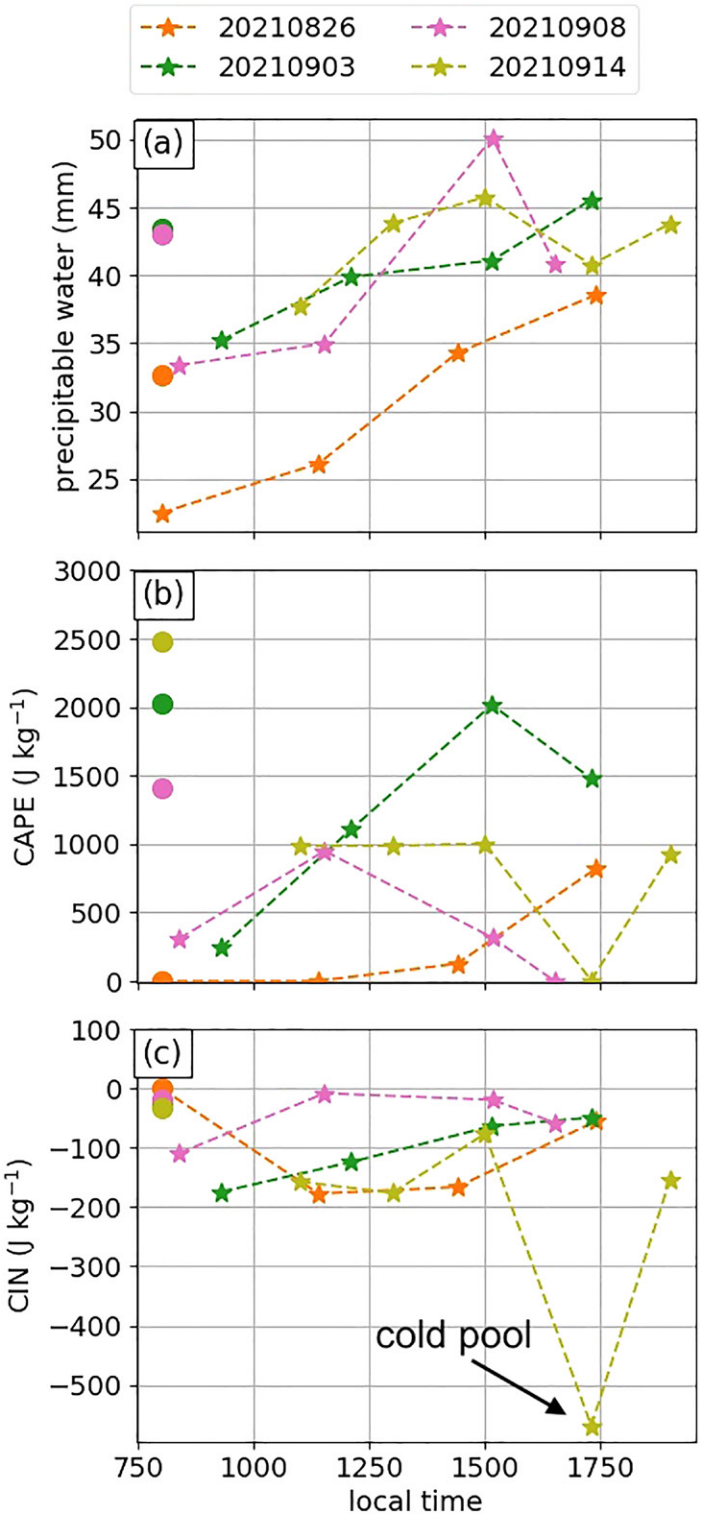

Fig. 7. Time series of (a) precipitable water, (b) CAPE, and (c) CIN derived from the UPRM soundings launched on 26 Aug (orange), 3 Sep (green), 8 Sep (pink), and 14 Sep (mustard). Stars represent derived values from the UPRM soundings, whereas circles represent derived values from the SJU soundings.

3 September event. We sampled another localized rainfall event on 3 September 2021. This event produced approximately 75 mm (3 in.) of rain over the northwestern municipalities of Puerto Rico (Fig. 8a). A weak easterly wave was present over the eastern Caribbean on this day (Fig. 3b). In contrast to the 26 August event, this one was associated with storms that propagated offshore as indicated by an elongated rainfall signature over the Atlantic waters north of Puerto Rico. Our team observed

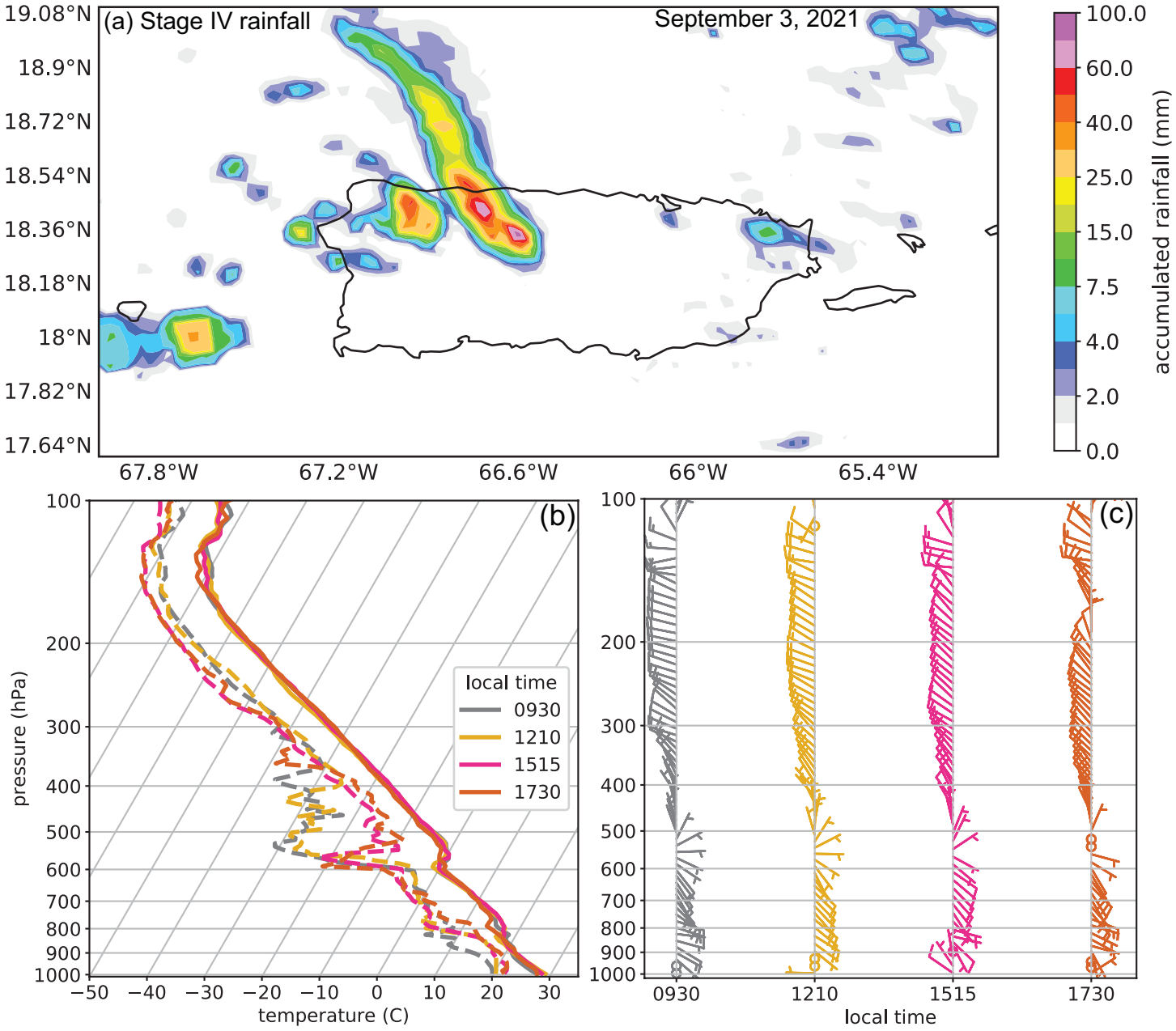

Fig. 8. As in Fig. 6, but for conditions observed during the 3 Sep event.

cumulonimbus clouds starting around 1300 LT on this day, and the radar-detected rainfall between 1400 and 1500 LT.

The soundings launched on this day show a slightly different synoptic configuration on this day than on 26 August (Fig. 8b). The morning (0900 LT) sounding shows two inversions: a relatively weak inversion around 800 hPa and a more pronounced inversion just above 600 hPa (just below 5 km AGL). Relatively dry conditions were present on this day as indicated by sounding-derived relative humidity values between 50% and 60% above 500 hPa and precipitable water of 35 mm (Fig. 7a). The vertical profile of winds was characterized by substantial directional shear given by low-level easterlies and upper-level westerlies (Fig. 8c). The near-surface winds suggest that the sea-breeze circulation was already starting by 0930 LT on this day given the near calm conditions.

The subsequent soundings show a different evolution during this day than on 26 August (Figs. 8b,c). By midday (1210 LT), the boundary layer had substantially warmed and moistened in comparison to the morning conditions. However, a pronounced inversion persisted

between 500 and 600 hPa and the middle troposphere remained relatively dry. A sea-breeze circulation was clearly established by now as indicated by near-surface westerlies of up to 5 kt (2 m s^{-1}) in the lowest 750 m AGL (Fig. 8c). The upper-tropospheric flow remained characterized by westerlies—an indication of the shallow nature of the sea-breeze circulation.

While the pronounced inversion and upper-tropospheric westerlies persisted through the afternoon hours, a substantial moistening happened in the middle troposphere between 400 and 600 hPa. The dewpoint temperatures measured by the 1515 LT had increased by 10°–15°C in comparison to the morning and noon soundings (Fig. 8b). Notably, the precipitable water increased at this time to approximately 41 mm and CAPE reached approximately 2,000 J kg^{-1} (Figs. 7b,c). Some inhibition remained—likely associated with the pronounced inversion—as the sounding-estimated CIN was approximately 50 J kg^{-1} at that time (Fig. 7c). Moreover, the near-surface westerlies strengthened to approximately 10 kt (5 m s^{-1}) likely indicating that the sea-breeze circulation was at its peak strength at this time (Fig. 8c). Further indication of this possibility is the near-surface calm condition sampled by the early evening sounding. By that time, the middle troposphere remained relatively moist but the surface cooled down diminishing the amount of instability.

Overall, our data suggest that boundary layer moistening and inland convergence aided by the sea breeze could have also contributed to the formation of storms on this day. Our team observed several short-lived convective cells leading up to the storms that produced rainfall in the afternoon. We hypothesize that those short-lived updrafts dissipated due to the exceptionally dry conditions, but at the same time those updrafts fluxed water vapor upward that helped to moisten the middle troposphere. Like on the 26 August event, the middle-tropospheric conditions were likely unfavorable for long-lived storms.

8 September event. A widespread rainfall event took place over Puerto Rico on 8 September 2021 (Fig. 9). Stage-IV estimates show a wide region of 15-mm accumulated rainfall with higher local amounts reaching up to 60 mm (2.5 in.) (Fig. 9a). Most of the rainfall on this day fell over the southwestern and western interior municipalities. This change in rainfall location—in comparison to the 26 August and 3 September events—was likely associated with a change in the synoptic flow over the island (Fig. 3c). The morning sounding from San Juan captured east-northeasterly flow on this day (not shown, but evident on the 0830 LT sounding from Mayagüez; Fig. 5d). Such flow could have focused the near-surface convergence and associated lift over southwestern Puerto Rico. We are investigating that possibility through a climatological analysis of rainfall location as a function of lower-tropospheric flow measured in San Juan.

The radiosonde measurements taken over western Puerto Rico show a slightly different scenario than in the first two events (Figs. 9b,c). The morning sounding showed several inversions from the surface up to 500 hPa (5 km AGL), a relatively moist boundary layer with relative humidity values around 70% below 800 hPa (lowest 1 km AGL), and relatively dry conditions aloft with relative humidity values below 50% in the middle troposphere. The measured winds were relatively weak (less than 5 kt, 2 m s^{-1}) in the lower troposphere and nearly calm within an extensive layer between 700 and 400 hPa. Aloft, the winds turned from northwesterlies to westerlies to easterlies between 300 and 100 hPa. These conditions were overall different than on the first two events.

As the day progressed, the air column over Mayagüez moistened up and became more unstable. The sounding-derived precipitable water reached 35 mm as indicated by the measurements taken around 1200 LT (Fig. 7a). CAPE more than doubled by this time as well—the morning sounding was associated with 350 J kg^{-1} of CAPE while that quantity was over 1,000 J kg^{-1} around noon (Fig. 7b). Such increase in instability was likely aided by a pronounced near-surface warming as indicated by temperatures of 30°C at the launch point of the radiosonde. Although the middle troposphere remained dry, the boundary layer

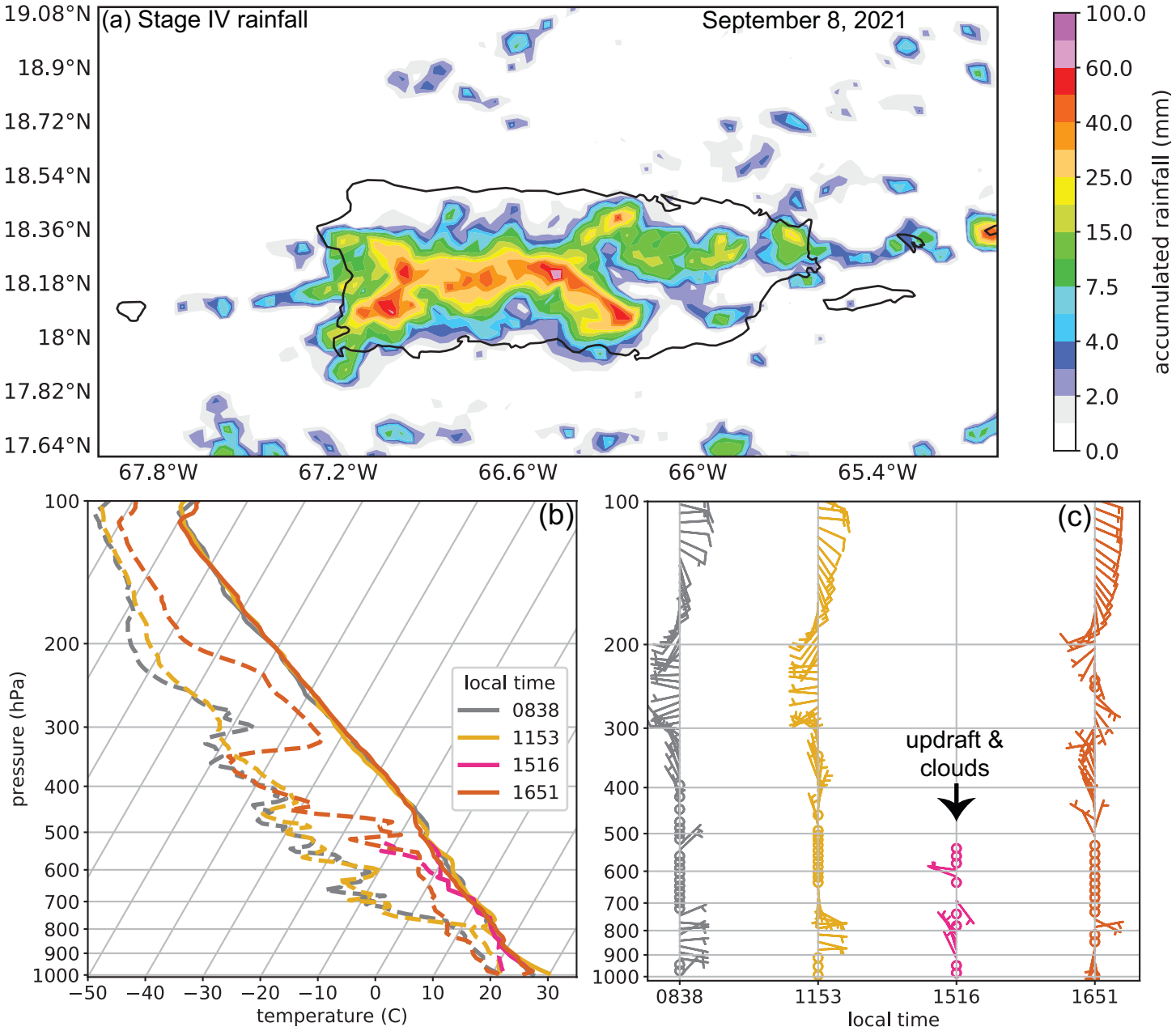

Fig. 9. As in Fig. 6, but for conditions observed during the 8 Sep event. The radiosonde launched at 1516 LT entered an updraft and associated clouds.

moistened up (as it did on other days) and the amount of CIN remained nearly negligible (Fig. 7c). Interestingly, there was no sign of onshore flow as the winds remained weak or near calm over Mayagüez.

Convection developed around 1300 LT and moved over our deployment site, preventing a sounding launch at 1400 LT. Our team sheltered in place due to substantial lightning in the region and a signature of rotating clouds above us. Instead, we launched a sounding when conditions allowed around 1516 LT. This sounding entered an updraft and traveled through some clouds as indicated by the 100% relative humidity (dewpoint matching the temperature) above 900 hPa (1 km AGL) (Fig. 9b). Below 1 km AGL, conditions had cooled down and moistened up as indicated by the temperature and dewpoint profiles. The wind profile shows weak northwesterlies around 800–900 hPa (1–2.5 km AGL), although those measurements are likely dominated by the storm circulation (Fig. 9c).

Following the storms, the early evening sounding sampled substantial boundary layer cooling and drying. The near-surface temperature returned to similar values as in the

morning, and the dewpoint temperature decreased to a minimum with respect to the samples we obtained on this day. The lower-to-middle troposphere moistened up substantially with sounding-derived relative humidity values of near 70% and precipitable water reaching 50 mm. However, CAPE values decreased to nearly 0 J kg^{-1} at this point likely as a result of several inversions and smaller lapse rates than earlier on this day. This reduction in instability—together with the diurnal influences—likely prevented the storms from continuing into the evening or from propagating offshore.

14 September event. Our last two events occurred on 13 and 14 September. Both days had similar characteristics; therefore, we will only summarize the 14 September event. This day was the most convectively active day of all days we sampled. Rainfall accumulations happened not only over the island but also over the local waters (Fig. 10a). Stage-IV estimates indicate that rainfall accumulations of over 15 mm (~0.5 in.) happened over most of the region, with a localized amount of approximately 75 mm (3 in.) over the western interior. Regions of precipitation oriented from southeast to northwest off northwestern Puerto Rico are associated with storms that initiated over land and propagated offshore.

This day was associated with the wettest and most unstable conditions that we recorded during our observational period. The morning radiosonde from San Juan measured approximately 50 mm of precipitable water and 2,479 J kg^{-1} of CAPE (Figs. 7a,b). Sounding-derived relative humidity values exceeded 50% at most levels—a substantial change from the other events. Evidently, there was also a noteworthy amount of CIN likely associated with the trade wind inversion around 800 hPa (Fig. 7c). Southeasterly winds were present over a layer from the surface up to 400 hPa (approximately 6 km AGL). Southerly and westerly winds dominated above 400 hPa. This configuration was influenced by the presence of an upper-tropospheric trough over Hispaniola, which induced anomalous lifting and moistening over Puerto Rico (according to the NWS weather discussion and Fig. 3d).

The progression of atmospheric conditions on this day had both similarities and differences to the observed progression during other days (Figs. 10b,c). The 1100 LT sounding shows that—like in other days—the boundary layer moistened and warmed up from its morning conditions. The sounding-derived precipitable water and CAPE were approximately 45 mm and 1,000 J kg^{-1}, respectively, over UPRM (Figs. 7a,b). These conditions persisted through the afternoon as indicated by the 1300 and 1500 LT soundings. Westerly-to-northwesterly winds were sampled over a shallow layer from the surface up to 900 hPa (lowest 1 km AGL) at 1100, 1300, and 1500 LT (Fig. 10c). Those winds are indicative of onshore flow associated with a clearly established sea-breeze circulation. Aloft, southeasterly winds persisted between 900 and 500 hPa and southerly flow also persisted above 500 hPa.

By 1500 LT, when storms had already formed over the western interior, the atmospheric column over Mayagüez had cooled and became near-saturated. Precipitable water exceeded 45 mm at this time, and the amount of CAPE remained at around 1,000 J kg^{-1} (Fig. 7). Sounding-derived relative humidity values approached saturation, especially in the boundary layer.

Storms were long lived and moved over our region on this day. We were unable to launch further soundings until conditions cleared up during the passage of a cold pool. The 1730 LT sounding sampled that cold pool (Fig. 10b). The near-surface temperature cooled down by 5°C from its earlier peak values and a pronounced inversion appeared around 800 hPa (between 1 and 2 km AGL). Such changes were associated with near-zero CAPE and the largest amount of CIN that we recorded (~575 J kg^{-1}) (Fig. 7c). The near-surface winds returned to easterlies especially between 900 and 600 hPa. Despite the passage of this cold pool, the lower and middle troposphere remained relatively moist with relative humidity values over 60%. Such moist conditions were likely aided by moist southerly flow above 500 hPa (Fig. 10c).

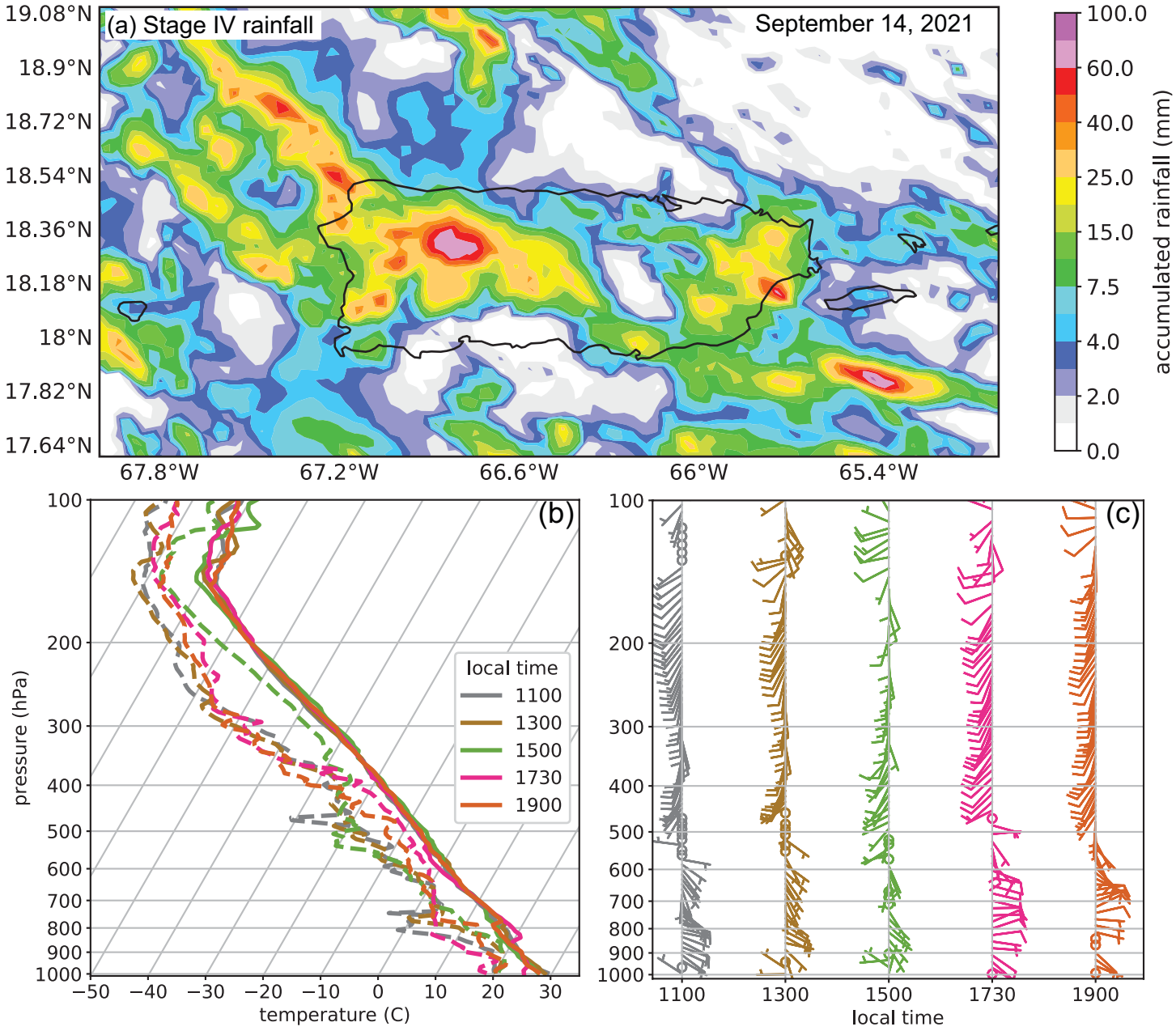

Fig. 10. As in Fig. 6, but for conditions observed during the 14 Sep event. The radiosonde launched at 1730 LT sampled a cold pool.

The last sounding of our project sampled the evening conditions, when storms were propagating offshore. The 1900 LT sounding indicates that the boundary layer had recovered from the cold pool by this time because the inversion weakened and moved up to a higher altitude (above 800 hPa or 2 km AGL) (Fig. 10b). Both precipitable water and CAPE values increased to near similar conditions observed during the early afternoon (Figs. 7a,b). East-southeasterly winds remained in place in the lower troposphere and southerly winds persisted above 500 hPa (Fig. 10c).

On this day, the greater moisture availability in combination with diurnal forcing and the sea-breeze circulation likely promoted convective development over most of the island. The background southeasterly flow likely aided in the boundary layer recovery from cold pools and moistening of the middle troposphere by continuously fluxing moist, warm air from lower latitudes toward Puerto Rico. At the same time, the upper-tropospheric trough likely provided an environment with prolonged lifting and moistening. Such conditions likely helped not only to trigger widespread storms during the day but also allowed storms to be long lived, to persist through the evening and nighttime hours, and to propagate offshore.

These findings are consistent with the diurnal cycle of rainfall over the Maritime Continent, which also tends to be enhanced on the leeward side of background wind imposed by the large-scale perturbations (Qian 2020; Bai and Schumacher 2022; Zhou et al. 2022). However, the precise mechanisms through which the large-scale winds enhance rainfall on the leeward side remain unclear and several mechanisms have been proposed, such as the wake effects, effects on land breeze, and gravity waves (e.g., Ruppert et al. 2020; Qian 2020; Bai and Schumacher 2022). The days with strong diurnal rainfall over tropical Pacific islands also tends to be associated with high humidity as seen on 13–14 September over Puerto Rico (Sakaeda et al. 2020; Natoli and Maloney 2021).

In contrast to the findings over the Maritime Continent, the results of the Dominica Experiments showed that the days with strong trade winds and its interaction with the topography provided mechanical forcing on heavy rainfall on the windward slope of the island instead of the leeward slope (Smith et al. 2012). This difference in the existence of orographically forced rainfall on the windward slope between Dominica and Puerto Rico indicates potential sensitivity to the differences in the island orientation, orography, and studied seasons. These studies highlight that all these hypotheses on the mechanisms that influence coastal rainfall remained to be tested with more detailed analyses and datasets.

Student engagement. Our project took place during the unprecedented and highly uncertain times of the global COVID-19 pandemic. CPEX-AW was originally planned to happen in Cape Verde during the months of July–August 2020. The campaign was delayed until 2021, and the main operations were moved to Saint Croix. These changes led our team to focus our scientific goals on the diurnal variations of coastal rainfall over western Puerto Rico. Our experimental design was informed by a project that the fourth author of this study had completed during her 2019/20 summer internships sponsored by the Significant Opportunities in Atmospheric and Related Sciences (SOARS). All these circumstances serendipitously led our team to establish a collaborative effort between our institutions and UPRM.

All radiosondes were launched by UPRM students with the guidance and mentorship of their professors and one of the scientific team members (Fig. 11). Twelve undergraduate students—all from different majors—participated in the project. Most of the students were part of the UPRM course FISI4999 (Physics Undergraduate Research). This course, taught by Héctor J. Jiménez and coauthor of this study, introduced the students to scientific research on topics related to atmospheric and related sciences. Several other students, who were members of the local AMS Student Chapter, were welcomed to participate based on their interest and availability.

On each day of radiosonde launches, the students were part of the sampling process from beginning to end. We first informed them a day ahead of time that weather forecasts were showing the possibility of a rainfall event. The students then participated in the entire process of preparing and launching a weather balloon—from preparing the different parts of the radiosonde system, to filling up the balloon with helium, to releasing the weather balloon. Once launched, the students were invited to monitor the incoming data in real time. If the radiosonde stopped transmitting data earlier than expected, the students then tried to find explanations for why it might have happened. On one such occasion, several students noted that the balloon trajectory coincided with a location of significant lightning activity. The students were always enthusiastic despite some launches happening early in the morning, during peak hot and windy conditions, or even at nighttime (Fig. 11).

We also encountered several challenges that merit mention here. The main challenge was coordinating the precise timing of radiosonde launches because the students were enrolled in different courses at different times. Most students also left campus to visit their families on the weekends, which limited the radiosonde launches to weekdays (with the exception of

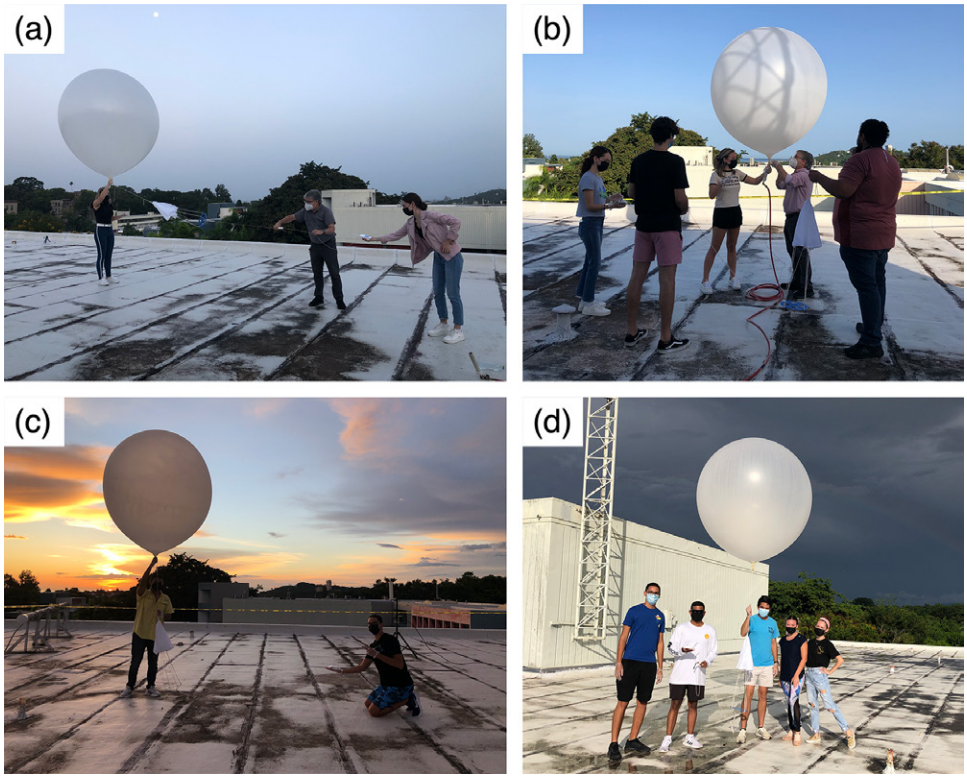

Fig. 11. UPRM students launched soundings during different times of the day to observe the diurnal cycle of rainfall over western Puerto Rico. Panels show some of the students launching radiosondes (a) after sunrise, (b) at midday, (c) at sunset, and (d) before an approaching afternoon storm.

4 September). Another noteworthy challenge was the wide range of students' backgrounds—from senior students who had participated in research projects to freshmen students who had never taken a course on meteorological instrumentation. We tried to alleviate this challenge by providing as much information as needed to inform the freshmen students while also engaging the senior students in leadership roles during each launch.

Nonetheless, the student engagement on this project proved to be valuable for both reaching our scientific objectives and, most importantly, for integrating their knowledge on our project. All student participants were local residents of Puerto Rico. They are the ones who experience the rainfall events on a daily basis. Many of them are also interested in pursuing careers in weather forecasting. Their input during the project was invaluable when adjusting the time of our launches—for example, we determined the time of the afternoon launches based on the students' recollection of the typical timing of rainfall over UPRM. Likewise, their learning experience throughout the course of the project led many of them to gain knowledge about when to expect long-lived storms that may affect their daily activities. Integrating the students on our project was also important because we engaged the local community instead of just conducting "parachute" or "helicopter" science—a term used to describe when scientists conduct field work without involving or connecting with the local residents (Adame 2021).

Following the completion of our project, most of the students expressed interest in continuing their careers in atmospheric sciences. We asked the students to share with us what they thought about their participation on the radiosonde launches. One of the students indicated: "I learned a lot, and reaffirmed my interests on becoming a research meteorologist." Another student said: "[I am] grateful to have had the opportunity to collaborate on this project at my university, UPRM. It was a very rewarding experience and training that definitely will help me in my future career as a meteorologist." A third student said: "Being a volunteer on this

project, gave me the opportunity to gain field work experience and helped me land my dream summer internship at NASA SARP [Student Airborne Research Project]." Just like this student, at least three others applied for and were accepted to summer internships. One of those students (Kevin Martínez) was accepted by the University of Oklahoma Research Experiences for Undergraduates (OU-REU) (Gonzalez-Espada and LaDue 2006) program. For his OU-REU project, Kevin analyzed the radiosonde data presented in this study in combination with other datasets to better understand the different rainfall events sampled during our project.

Areas of future research

The data collection component of our project opened many doors for research opportunities on the sensitivity of coastal rainfall to the compound interactions between the diurnal cycle, sea-breeze circulations, topography, and synoptic conditions. Our team will seek to better understand why some storms are able to form over western Puerto Rico and propagate offshore (such as in the 14 September event), while other storms quickly dissipate when they move over water (such as in the 3 September event). Another area that our team will explore is the influence of background flow on the location of peak convergence and its influence on the location of rainfall activity. Our observations suggest that east-northeasterly winds likely result on peak lower-tropospheric convergence (between the synoptic flow and the onshore flow associated with sea-breeze circulations) on southwestern Puerto Rico (like on 8 September) while southeasterly flow likely results on peak convergence farther north (like on 14 September).

Our data collection and analysis was limited to the time period and resources available during CPEX-AW. Atmospheric conditions were exceptionally dry during the first 2 weeks, which limited the number of events we could sample. At the same time, it is possible that our time period was affected by interannual variability of the tropical atmosphere. For future projects, we recommend a multiyear effort to minimize risks of not sampling enough events while also sampling conditions during different phases of interannual variability (e.g., El Niño, La Niña). We also recommend sampling more events and launching radiosondes at fixed times every day (weather permitting) to allow for a statistical comparison among different events.

Additionally, this project motivates new questions regarding weather forecasting and numerical weather prediction. Our observations show distinct diurnal evolution of the boundary layer and middle troposphere that can lead to rainfall accumulations even on days with dry conditions associated with Saharan dust outbreaks. Yet it is unclear if numerical weather prediction models are able to capture such evolution. At the same time, it is also unclear what kind of model grid spacing (both vertical and horizontal) would be necessary to capture the fine details of compound interactions between the diurnal cycle, sea-breeze circulations, topography, and synoptic conditions. A future study pursue these topics by, for example, comparing the diurnal evolution of atmosphere conditions on MPAS-A, or by producing sensitivity experiments with different model configurations and altered topography.

Last, we are interested in possibly generalizing our results for other coastal regions. Puerto Rico exhibits some unique features such as having an east–west-oriented mountain range. However, it is possible that our findings on what leads to short-lived versus long-lived storms could be applicable to rainfall patterns on other islands or coastal regions. Likewise, we are interested in understanding how storms propagate offshore over more expansive coastal regions such as western Africa. Over that region, mesoscale convective systems produce a substantial amount of rainfall over water rather than over land—a clear difference from our observations over western Puerto Rico (Hamilton et al. 2017). A follow-up field project (called CPEX-Cape Verde or CPEX-CV) sponsored by NASA will address this and other questions through targeted observations within and around convective systems near coastal Africa.

Acknowledgments. We are incredibly grateful to the late Dr. Gail Skofronick-Jackson, who was the NASA Project Manager for CPEX-AW, for supporting our radiosonde project. We are also indebted to all the UPRM students, UPRM professors, and NCAR scientists who contributed, one way or another, to the successful launch of our radiosondes. Many thanks also to the weather forecasters of the National Weather Service San Juan Office who provided forecasts, guidance, and feedback for our project. Comments from four anonymous reviewers helped improve this manuscript. This work was funded by NASA under Grant 80NSSC20K0901. The first author acknowledges that this material is based upon work supported by NCAR, which is a major facility sponsored by the National Science Foundation under Cooperative Agreement 1852977.

Data availability statement. All data from the CPEX-AW campaign are publicly available through NASA's Atmospheric Science Data Center at https://doi.org/10.5067/CPEXAW/DATA101 as cited in Jackson (2022). The NWS San Juan sounding data are publicly available through the Integrated Global Radiosonde Archive (Durre et al. 2018).

References

Adame, F., 2021: Meaningful collaborations can end "helicopter research." *Nature*, https://doi.org/10.1038/d41586-021-01795-1.

Bai, H., and C. Schumacher, 2022: Topographic influences on diurnally driven MJO rainfall over the Maritime Continent. *J. Geophys. Res. Atmos.*, **127**, e2021JD035905, https://doi.org/10.1029/2021JD035905.

Biasutti, M., S. E. Yuter, C. D. Burleyson, and A. H. Sobel, 2012: Very high resolution rainfall patterns measured by TRMM Precipitation Radar: Seasonal and diurnal cycles. *Climate Dyn.*, **39**, 239–258, https://doi.org/10.1007/s00382-011-1146-6.

Christopoulos, C., and T. Schneider, 2021: Assessing biases and climate implications of the diurnal precipitation cycle in climate models. *Geophys. Res. Lett.*, **48**, e2021GL093017, https://doi.org/10.1029/2021GL093017.

Dias, J., M. Gehne, G. N. Kiladis, N. Sakaeda, P. Bechtold, and T. Haiden, 2018: Equatorial waves and the skill of NCEP and ECMWF numerical weather prediction systems. *Mon. Wea. Rev.*, **146**, 1763–1784, https://doi.org/10.1175/MWR-D-17-0362.1.

Dirmeyer, P. A., and Coauthors, 2012: Simulating the diurnal cycle of rainfall in global climate models: Resolution versus parameterization. *Climate Dyn.*, **39**, 399–418, https://doi.org/10.1007/s00382-011-1127-9.

Durre, I., X. Yin, R. S. Vose, S. Applequist, and J. Arnfield, 2018: Enhancing the data coverage in the Integrated Global Radiosonde Archive. *J. Atmos. Oceanic Technol.*, **35**, 1753–1770, https://doi.org/10.1175/JTECH-D-17-0223.1.

Fernández-Alvarez, J. C., R. Sorí, A. Pérez-Alarcón, R. Nieto, and L. Gimeno, 2020: Affectation and rainfall contribution of tropical cyclones in Puerto Rico from 1980 to 2016. *Environ. Sci. Proc.*, **4**, 30, https://doi.org/10.3390/ecas2020-08130.

Gonzalez-Espada, W. J., and D. S. LaDue, 2006: Evaluation of the impact of the NWC REU program compared with other undergraduate research experiences. *J. Geosci. Educ.*, **54**, 541–549, https://doi.org/10.5408/1089-9995-54.5.541.

Hamilton, H. L., G. S. Young, J. L. Evans, J. D. Fuentes, and K. M. Nez Ocasio, 2017: The relationship between the guinea highlands and the West African offshore rainfall maximum. *Geophys. Res. Lett.*, **44**, 1158–1166, https://doi.org/10.1002/2016GL071170.

Hersbach, H., and Coauthors, 2020: The ERA5 global reanalysis. *Quart. J. Roy. Meteor. Soc.*, **146**, 1999–2049, https://doi.org/10.1002/qj.3803.

Jackson, G. S., 2022: Convective Processes Experiment—Aerosols and Winds (CPEX-AW) field campaign collection. NASA Global Hydrometeorology Resource Center DAAC, accessed 1 March 2022, https://ghrc.nsstc.nasa.gov/uso/ds_details/collections/cpexawC.html.

Jury, M. R., 2022: Inter-comparison of past and projected climatic trends in Puerto Rico: 1950–2100. *J. Water Climate Change*, **13**, 2713–2724, https://doi.org/10.2166/wcc.2022.071.

——, and S. Chiao, 2013: Leeside boundary layer confluence and afternoon thunderstorms over Mayaguez, Puerto Rico. *J. Appl. Meteor. Climatol.*, **52**, 439–454, https://doi.org/10.1175/JAMC-D-11-087.1.

——, ——, and E. W. Harmsen, 2009: Mesoscale structure of trade wind convection over Puerto Rico: Composite observations and numerical simulation. *Bound.-Layer Meteor.*, **132**, 289–313, https://doi.org/10.1007/s10546-009-9393-3.

Kikuchi, K., and B. Wang, 2008: Diurnal precipitation regimes in the global tropics. *J. Climate*, **21**, 2680–2696, https://doi.org/10.1175/2007JCLI2051.1.

Larsen, M. C., 2000: Analysis of 20th century rainfall and streamflow to characterize drought and water resources in Puerto Rico. *Phys. Geogr.*, **21**, 494–521, https://doi.org/10.1080/02723646.2000.10642723.

Martin, C., and I. Suhr, 2021: NCAR/EOL Atmospheric Sounding Processing Environment (ASPEN) software, version 3.4.5. NCAR/EOL, www.eol.ucar.edu/content/aspen.

Natoli, M. B., and E. D. Maloney, 2021: Quasi-biweekly extensions of the monsoon winds and the Philippines diurnal cycle. *Mon. Wea. Rev.*, **149**, 3939–3960, https://doi.org/10.1175/MWR-D-21-0208.1.

Qian, J.-H., 2020: Mechanisms for the dipolar patterns of rainfall variability over large islands in the Maritime Continent associated with the Madden–Julian oscillation. *J. Atmos. Sci.*, **77**, 2257–2278, https://doi.org/10.1175/JAS-D-19-0091.1.

Ruppert, J. H., X. Chen, and F. Zhang, 2020: Convectively forced diurnal gravity waves in the Maritime Continent. *J. Atmos. Sci.*, **77**, 1119–1136, https://doi.org/10.1175/JAS-D-19-0236.1.

Sakaeda, N., G. Kiladis, and J. Dias, 2020: The diurnal cycle of rainfall and the convectively coupled equatorial waves over the Maritime Continent. *J. Climate*, **33**, 3307–3331, https://doi.org/10.1175/JCLI-D-19-0043.1.

Skamarock, W. C., J. B. Klemp, M. G. Duda, L. D. Fowler, S.-H. Park, and T. D. Ringler, 2012: A multiscale nonhydrostatic atmospheric model using centroidal Voronoi tessellations and C-grid staggering. *Mon. Wea. Rev.*, **140**, 3090–3105, https://doi.org/10.1175/MWR-D-11-00215.1.

Smith, R. B., and Coauthors, 2012: Orographic precipitation in the tropics: The Dominica Experiment. *Bull. Amer. Meteor. Soc.*, **93**, 1567–1579, https://doi.org/10.1175/BAMS-D-11-00194.1.

Villamil-Otero, G., R. Meiszberg, J. S. Haase, K.-H. Min, M. R. Jury, and J. J. Braun, 2015: Topographic–thermal circulations and GPS-measured moisture variability around Mayaguez, Puerto Rico. *Earth Interact.*, **19**, https://doi.org/10.1175/EI-D-14-0022.1.

Watters, D., A. Battaglia, and R. P. Allan, 2021: The diurnal cycle of precipitation according to multiple decades of global satellite observations, three CMIP6 models, and the ECMWF reanalysis. *J. Climate*, **34**, 5063–5080, https://doi.org/10.1175/JCLI-D-20-0966.1.

Yang, G.-Y., and J. Slingo, 2001: The diurnal cycle in the tropics. *Mon. Wea. Rev.*, **129**, 784–801, https://doi.org/10.1175/1520-0493(2001)129<0784:TDCITT>2.0.CO;2.

Zhou, Y., S. Wang, and J. Fang, 2022: Diurnal cycle and dipolar pattern of precipitation over Borneo during an MJO event: Lee convergence and offshore propagation. *J. Atmos. Sci.*, **79**, 2145–2168, https://doi.org/10.1175/JAS-D-21-0258.1.

Zipser, E. J., 1977: Mesoscale and convective-scale downdrafts as distinct components of squall-line structure. *Mon. Wea. Rev.*, **105**, 1568–1589, https://doi.org/10.1175/1520-0493(1977)105<1568:MACDAD>2.0.CO;2.